Study of Defects in LEC-grown Undoped SI-GaAs by Thermally Stimulated Current Spectroscopy

ZHAOQIANG FANG, LEI SHAN, T. E. SCHLESINGER and A. G. MILNES

Carnegie Mellon University, Pittsburgh, PA 15213 (U.S.A.)

(Received in revised form August 29, 1989)

Abstract

Thermally stimulated current spectroscopy (TSC) reveals at least six traps in LEC semi-insulating GaAs. The relative concentrations of the traps are related to the native defect complexes expected from growth stoichiometry and subsequent annealing conditions. Variations of the sample conditions prior to the TSC scan are found to provide some evidence as to the nature of the traps observed and also appear to cause photo-induced defect reactions.

1. Introduction

Native defects in LEC-grown (liquid-encapsulated Czochralski) undoped semi-insulating (SI)-GaAs play an important role in its semi-insulating properties (involving compensation of EL2), the luminescence lifetime, and in field effect transistor device performance (such as voltage threshold variation due to the inhomogeneous distribution of these native defects) [1-3]. A universally agreed model of EL2, the main native defect in SI-GaAs, has not yet been established although several techniques have been applied to study these antisite-related defect complexes that involve arsenic on a gallium site [4]. Other native defects, such as Ga_{As}, V_{As}, V_{Ga}, As_i and their complexes have been examined by investigating their occurrence under different growth and annealing conditions. Techniques used include temperature-dependent Hall effect (TDH), deep level transient spectroscopy (DLTS) and photoluminescence (PL) measurements [5].

In this paper thermally stimulated current (TSC) [6–8] is shown to be very suitable for trap studies in semi-insulating GaAs materials, although subject to certain limitations that we discuss. Suitable sample preparation and measurement conditions are first described. The metalization technique we used allowed the study of as-grown

defects in SI-GaAs, since no heat treatment was involved. We present observations related to samples with different stoichiometries and annealing treatments. Measurement conditions examined included the effects of biasing polarity changes, light intensity variations, the illumination time at 90 K, the starting temperature (from which the sample is cooled down to 90 K after a previous run of a TSC measurement) and the waiting time between interrupting illumination and starting the thermal scan. The results allow us to speculate as to the identity of four main traps (T_2, T_3, T_5) and T_6 0 observed in the TSC spectra of bulk GaAs.

2. Experimental technique and measurement conditions

The Schottky barrier structure used in the photo-induced transient spectroscopy (TSC) measurements was the same as that used in PITS measurements [9]. Thin circular dots of Au-Ge or gold (about 500 Å thick and 0.7 mm in diameter) were deposited on the front face of each sample, of thickness about 400 μ m, by thermal evaporation through a metal mask under high vacuum. Before evaporation the samples were degreased with organic solvents and etched with H_2SO_4 : H_2O_2 : H_2O (5:1:1 by volume) to remove a surface layer of a few micrometers. The sample was usually LEC semi-insulating material in the as-grown, or ingot-annealed, condition. Some samples, however, had been silicon implanted and annealed and the activation efficiency determined. The implanted layer was removed in the etching process before TSC measurements. The samples were mounted on a TO-5 header with silver epoxy on the opposite face and the asdeposited contacts were wire bonded by ultrasonic bonding. As-deposited contacts with this sandwich geometry structure were found to show larger photocurrents at lower temperatures than alloyed contacts and quite small dark currents at elevated temperatures (up to 250 K), which leads to a sensitive TSC measurement. Since the SI-GaAs sample experiences no significant heat treatment during evaporation of the thin Au-Ge or gold layer for the as-deposited contact, it is assumed that the native defects in as-grown SI-GaAs survive unchanged and can be characterized. The TO-5 header with sample was mounted on a liquid nitrogen cooled finger in a cryostat with a quartz window. A copper-constantin thermocouple was fixed on the finger close to the TO-5 header. Above-bandgap excitation light of a range of intensities was provided by a He-Ne laser (1.96 eV, 7.5 mW), through an attenuator. The excitation spot was adjusted by a lens to be larger than the as-deposited metal dot. The thermally stimulated currents were measured by a Keithley Model 616 electrometer. The TSC and temperature data were stored and processed by an HP 9836 computer through a digital multimeter (HP 3478A) and a system voltmeter (HP 3437A). To eliminate any moisture on the sample surface the sample was first baked at about 100 °C for 15 min in the cryostat and then cooled down to the lowest temperature (about 90 K). When the photocurrent at around 90 K reached a stable value after sufficient illumination time (greater than 10 min), the thermal scan with an average heating rate from 0.1 K s⁻¹ to 0.3 K s⁻¹ was started and the TSC spectrum was recorded for the temperature range 90 to 250 K. At temperatures above 250 K the increase in dark current, which is due to the thermal ionization of electrons from the main deep donor (EL2), did

not allow the observation of very deep traps. The sample was usually warmed up to about 100 °C and cooled down again for the next measurement run (to ensure uniform starting conditions). In TSC measurements, the d.c. current which corresponds to the thermal release of carriers from traps is recorded as a function of temperature after only one optical excitation at low temperature. Therefore the conditions reported for TSC measurement should include (1) the energy of optical excitation, (2) the illumination temperature and (3) the heating rate, on which the position and height of a TSC peak are dependent [10]. Other conditions, however, are also found to have a significant effect on the TSC spectrum. They include (4) the biasing polarity, (5) the illumination time, (6) the starting temperature, from which the sample is cooled down to about 90 K after a previous run of TSC measurement, (7) the waiting time between the interruption of the light excitation and the start of the thermal scan and (8) the intensity of light excitation. The behavior when conditions (4)-(8) are varied provides useful information that in general has not been available before.

The samples used in the study were taken from undoped SI-GaAs ingots prepared by both high pressure LEC and low pressure LEC, and from different melt stoichiometries (*i.e.* arsenic-rich and gallium-rich growth melts). A post-growth thermal process had been applied by the manufacturer to the as-grown SI-GaAs ingots in order to reduce stress and improve homogeneity in all the crystals [10]. To investigate the effect of further anneal on the traps, two samples were given wafer anneals before the TSC measurements.

TABLE 1 Summary of samples used in the study

Samples	Growth technique	Melt stoichiometry	Thermal history	Electrical pro	Si implant ^b activation (Ω /□)	
				ρ (ohm cm)	$\frac{\mu}{(cm^2 (V s)^{-1})}$	$(Si^{28}, 150 \text{ KeV}, 3 \times 10^{12} \text{ cm}^{-2})$
066ª	HP-LEC	As-rich	As-grown	5.6×10^{7}	6970	904
098	LP-LEC	Less As-rich	As-grown	3×10^{8}	5000	2263
113	HP-LEC	As-rich	As-grown	1.3×10^{7}	6890	780
059	HP-LEC	Ga-rich	As-grown	4.7×10^{7}	6690	1010
055ª	HP-LEC	As-rich	As-grown + wafer anneal (850 °C, 0.5 h in arsenic over- pressure ambient)	$> 1 \times 10^7$		904
066 A ^a	HP-LEC	As-rich	As-grown + wafer anneal (695 °C, 51 h	$>1\times10^7$		
098 A	LP-LEC	Less As-rich	in H ₂ flow)	$> 1 \times 10^{7}$		

^aSamples 066, 055 and 066 A are taken from same ingot but with different thermal history.

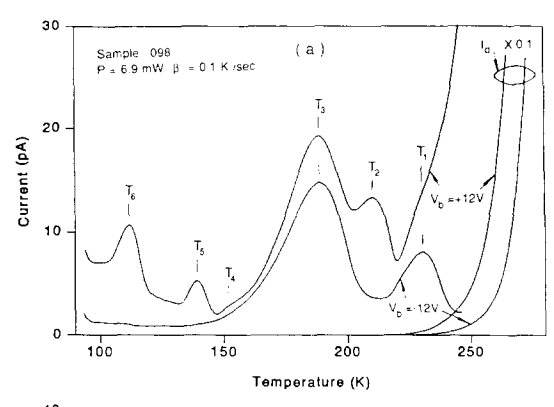
^bFrom measurements on adjacent wafers of the same ingot.

One annealed sample was obtained from a siliconimplanted and activated sample by removing the silicon-implanted layer. For activation the sample underwent capless annealing at 850 °C for 0.5 h in an arsenic overpressure ambient. The second sample underwent proximity annealing (two specimens placed face to face) at 695 °C for 51 h with hydrogen flow. The conditions for growth and annealing for all samples are listed in Table 1 together with some information about the electrical properties and the silicon implant activation.

3. Results and discussion

3.1. Typical TSC spectra and assignment of trap type

Figures 1(a) and 1(b) show typical TSC spectra for both biasing polarities for two as-grown SI-GaAs samples (098 and 066). The dark currents for the two biasing polarities are also shown. At least six traps designated T₁-T₆ can be observed in the temperature range 90-250 K. In terms of the usual criterion for the assignment of type to



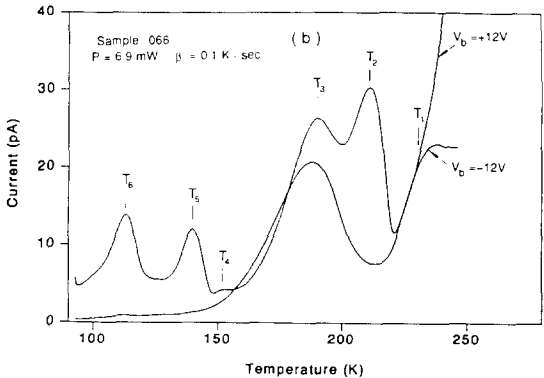


Fig. 1. TSC spectra for two semi-insulating GaAs specimens for the two directions of bias voltage: (a) sample 098, (b) sample 066. The dark currents for the two bias directions are also shown in (a). T_2 , T_4 , T_5 and T_6 are considered to be hole traps and T_1 to be an electron trap.

traps using intrinsic light and changing bias polarities [11, 12], T_2 , T_4 , T_5 and T_6 are hole traps and T_1 is an electron trap. T_3 cannot be assigned simply as a hole or electron trap since it appears in both biasing polarities with a small peak shift, as shown in Fig. 1(b). Its behavior will be discussed later.

3.2. The energy level and density of main traps

The maxima of a curve of thermally stimulated current *vs.* temperature can be correlated with the energy level of the trap while the trap densities can be obtained from the area under the curve. According to Bube [13],

$$E_i = kT_{\rm m} \ln \frac{N\sigma v k T_{\rm m}^2}{\beta E_i} \tag{1}$$

where E_i is the energy level of a given trap, $T_{\rm m}$ the temperature at the current peak, N the effective density of states, σ the capture cross-section, v the thermal velocity of carriers, k Boltzmann's constant, and β the heating rate during the thermal scan. The parameters N, v and σ are temperature dependent and related to carrier type. Two methods can be used for the determination of the energy level of a trap. Since eqn. (1) can be rearranged as

$$\frac{\ln T_{\rm m}^2}{\beta} = \frac{E_i}{kT_{\rm m}} - \ln \frac{Nv\sigma k}{E_i} \tag{2}$$

 E_i can be determined from the Arrhenius plot of $\ln T_{\rm m}^2/\beta$ vs. $1/T_{\rm m}$. Alternatively, with the temperature dependence of N and v considered, eqn. (1) becomes

$$E_{i} = kT_{m} \left(\ln \frac{T_{m}^{4}}{\beta} + \ln \frac{2 \times 10^{16} \sigma_{n}}{E_{i}} \right)$$
 (3)

or

$$E_{i_{=kT}^{\mathbf{m}}}\left(\ln\frac{T_{\mathbf{m}}^{4}}{\beta} + \ln\frac{1 \times 10^{17}\sigma_{\mathbf{p}}}{E_{i}}\right) \tag{4}$$

for electron traps and hole traps respectively. For $T_{\rm m} > 100$ K and with most reasonable values of $\sigma_{\rm n}$ or $\sigma_{\rm p}$, the first term in eqns. (3) or (4) dominates the second [14] and E_i can be calculated approximately using

$$E_i = kT_{\rm m} \ln \frac{T_{\rm m}^{-4}}{\beta} \tag{5}$$

The TSC spectra for sample 098 at four different heating rates are shown in Fig. 2. The TSC measurements were also performed with belowbandgap light $(E_{ex} = 1.15 \text{ eV})$ using alloyed Au-Ge contacts. As very similar spectra were obtained, we conclude that the traps observed by the 1.96 eV light (penetration depth about 0.3 μ m) are essentially bulk traps. The energy levels for the traps T_2 , T_3 , T_5 and T_6 are determined by Arrhenius plots to be 0.49 eV, 0.44 eV, 0.26 eV and 0.21 eV respectively. The approximate calculation, eqn. (5), provides energy levels for T_2 , T_3 , T_5 and T_6 of 0.44 eV, 0.39 eV, 0.26 eV and 0.20 eV respectively. The difference in the value of energy levels for T₂ and T₃ determined by the two methods is a result of the contribution of the second term in eqns. (3) and (4) in the calculation. Uncertainty in the measurement of the tempera-

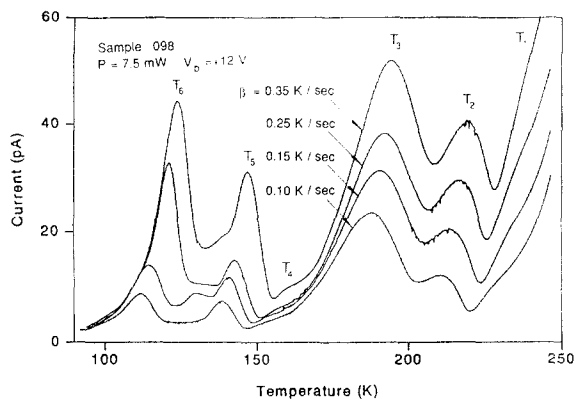


Fig. 2. TSC spectra for different heating rates in the range $0.1\text{--}0.35~\text{K s}^{-1}$. The high peaks correspond to high heating rates but the charge emission under each peak remains fairly independent of the heating rate.

ture of the sample will also contribute to the variation in the determined values of the energy levels of the trap. However, the peak temperatures $T_{\rm m}$ in this study are quite close to the data seen in the literature as seen in Table 2. It should be noted that from Table 2 different methods used for the determination of trap depths result in different values, although nearly the same peak temperatures were obtained by the various authors. For this reason comparison with the energies of the EL or HL traps given by Martin et al. [17] and Mitonneau et al. [18] is difficult. However, information obtained by changing the measurement conditions and using different samples with different stoichiometries and different annealing conditions will help us to speculate on the possible nature of the main traps in SI-GaAs.

In TSC, characterization of the density of traps $N_{\rm T}$ can be determined very approximately from the charge emitted, given by the area (current × time) of the emission hump divided by the effective volume of the crystal that may be regarded as having completely filled traps. With above-bandgap excitation the carrier generation will be restricted to a small fraction of the total volume. Allowing for a diffusion length of a few micrometers the effective depth and volume may be estimated to be about 10^{-2} of the total depth or volume. The estimated trap densities for the four main traps T₂, T₃, T₅ and T₆ for different samples are shown in Table 3, and are in the mid-10¹⁵ to 10¹⁷ cm⁻³ range. Studies of the TSC emission charge with below-bandgap excitation with a longer penetration depth indicated rather similar trap densities.

TABLE 2 Survey of TSC studies for semi-insulating GaAs

Methods	Samples	Excitation	TSC peaks/Trap depths (K eV - 1)							
a	HB-grown GaAs:O	Intrinsic or extrinsic light	95 0.15	111	126 0.22	141 0.25	156 0.28	191 0.35	212 0.45	250 0.53
и	HB-grown GaAs:Cr	Extrinsic light		_	124 0.21	141 0.24	156 0.28	191 0.35	212 0.46	250 0.53
h	LEC-grown SI-GaAs	Intrinsic light $E_{\rm ex} > 1.77 \text{ eV}$	92 0.24		124 0.33	141 0.35	0.39	192 0.43		238 0.50
h c	LEC-grown SI-GaAs LEC-grown	Intrinsic light $E_{\rm ex} > 1.77 \text{ eV}$ Intrinsic light	94 0.24 97	118 0.31 114	125	142 0.35 140	161 0.39 151	200 0.44 189	218 0.46 210	233
	a a b	HB-grown GaAs:O HB-grown GaAs:Cr LEC-grown SI-GaAs LEC-grown SI-GaAs	HB-grown Intrinsic or GaAs:O extrinsic light HB-grown Extrinsic light GaAs:Cr $E_{\rm ex}=0.86~{\rm eV}$ LEC-grown Intrinsic light SI-GaAs $E_{\rm ex}>1.77~{\rm eV}$	HB-grown Intrinsic or 95 GaAs:O extrinsic light 0.15 HB-grown Extrinsic light 10 GaAs:Cr $E_{\rm ex} = 0.86 {\rm eV}$ 0.1 LEC-grown Intrinsic light 92 SI-GaAs $E_{\rm ex} > 1.77 {\rm eV}$ 0.24 LEC-grown Intrinsic light 94 SI-GaAs $E_{\rm ex} > 1.77 {\rm eV}$ 0.24 LEC-grown Intrinsic light 94 LEC-grown Intrinsic light 97	$\begin{array}{cccccccccccccccccccccccccccccccccccc$	$\begin{array}{c ccccccccccccccccccccccccccccccccccc$				

^aThe trap depths were estimated from $E_i = 24 kT_m$.

^bThe trap depths were obtained using the equation $E_t = kT_m \ln(e\mu_c N_c/\sigma_m)$ where k, e, N_c and μ_c are Boltzmann's constant, electronic charge, effective density of states of the conduction band, and electron mobility, respectively. T_m is the temperature for neak TSC and σ_c is the conductivity at T_c

peak TSC and $\sigma_{\rm m}$ is the conductivity at $T_{\rm m}$. ^cThe trap depths were estimated from $E_i = kT_{\rm m} \ln T_{\rm m}^{-4}/\beta$.

Sample	T_2		T_3		T_{5}		T_o	
	$Q = (\mathbf{pA} \mathbf{s})$	$\frac{N_r}{(\text{cm}^{-3})}$	<i>Q</i> (pA s)	$\frac{N_t}{(cm^{+3})}$	$\frac{Q}{(pA s)}$	N ₁ (cm ⁻³)	$\frac{Q}{(pA s)}$	$\frac{N_t}{(\text{cm}^{-3})}$
066	3685	2×10 ¹⁶	****		885	4.8×10^{15}	836	4.5×10^{16}
098			7700	4.2×10^{16}	808	4.4×10^{15}	642	3.5×10^{15}
113	4576	2.5×10^{16}			856	4.6×10^{15}	840	4.5×10^{15}
059			17280	9.4×10^{16}	1748	9.5×10^{15}	2282	1.2×10^{15}

TABLE 3 Estimated trap density from TSC charge emission

The traps are believed to be native defects because of the dependencies on stoichiometry and because the impurity analysis of typical undoped SI-GaAs indicates that the concentrations of copper, iron and manganese measured by spark source mass spectrography are as low as 0.01, 0.02 and 0.005 ppma respectively [19].

3.3. The effect of stoichiometry

The electrical properties of high purity GaAs LEC-grown in pyrolytic boron nitride crucibles can be controlled by the melt composition which is represented by the fraction of arsenic atoms, f, in the melt. There exists a critical melt composition, $f_c = 0.475$, above which GaAs is SI or very slightly n type with EL2 or EL6 the dominant donor [20, 21] and below which it is markedly p type, with C_{As} or Ga_{As} the dominant acceptor [20]. TSC spectra for SI-GaAs samples grown under different stoichiometric conditions are presented in Figs. 3 and 4. Figure 3 shows two TSC spectra, one for sample 113, which was taken from a slightly arsenic-rich melt-grown ingot and the other for sample 059 which was taken from a slightly gallium-rich melt-grown ingot. Both ingots were grown by the high pressure (HP-) LEC technique. Figure 4 shows two other TSC spectra, one for sample 066, which was taken from an ingot with a diameter of 3 in, grown by the HP-LEC technique, and which revealed good silicon-implant activation efficiency, and the other for sample 098, which was taken from an ingot with a diameter of 2 in, grown by the low pressure (LP-) LEC technique, and which showed a poor Si-implant activation efficiency. It is assumed that the melt for the growth of the 3 in HP-LEC ingot was richer in arsenic than the melt for the growth of the 2 in LP-LEC ingot since the higher ambient pressure in the HP-LEC technique reduces arsenic loss from the melt. Trap T_2 dominates trap T_3 in the samples with an arsenic-rich stoichiometry and

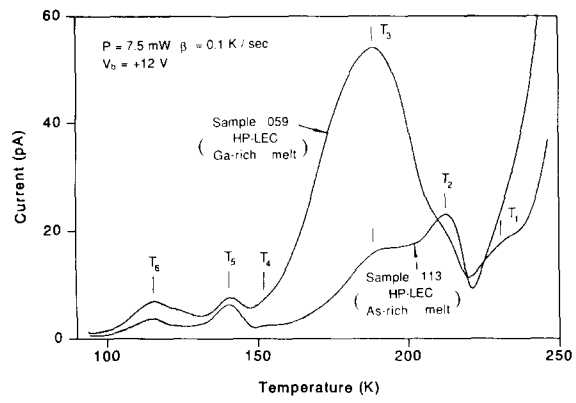


Fig. 3. Spectra for specimens from gallium-rich and arsenic-rich melts suggest that T_3 may be a defect related to arsenic vacancies.

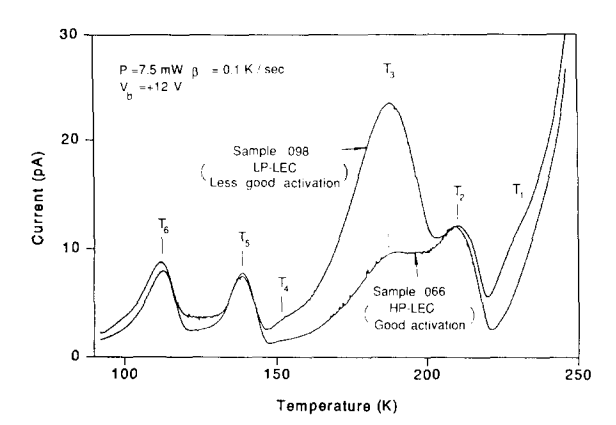


Fig. 4. Wafers with poorer activation efficiency for siliconimplanted atoms tend to show a high density of T₃. Presumably the high density of arsenic-vacancy-related traps allows more silicon to end up on arsenic sites.

trap T_3 dominates the trap T_2 in the samples with gallium-rich stoichiometry. This suggests that T_2 is related to V_{Ga} defects and T_3 is related to V_{As} defects. Single V_{Ga} defects are probably not stable at room temperature [22] and with interstitial arsenic convert to As_{Ga} . From eqn. (5) an energy level for T_2 of 0.44 eV is obtained. However, this becomes 0.54 eV after a capture cross-section correction is included using eqn. (4) and an esti-

mated $\sigma_{\rm p}$ of 10^{-15} cm². These values are very close to the energy level of As_{Ga}^{++} [23], and so the trap T_2 is tentatively identified to be the doubly ionized antisite defect As_{Ga}; the core of EL2. For trap T_3 (0.40 eV) we have two options: one is V_{As} according to the work of Thomas *et al.* [24], who found that LEC GaAs grown in a gallium-rich melt was n type provided that boron concentrations were kept low and they obtained an activation energy of 0.45 eV by temperaturedependent Hall measurements. The other possibility is that T_3 is $(Ga_{As}-V_{Ga})$ where V_{As} has been transformed by a nearest neighbor hop of gallium. Such traps are expected from the studies of Wagner and Van Vechten [25] and of Baraff and Schluter [26].

The appearance of T_3 in both positively and negatively biased TSC spectra (see Figs. 1(a) and 1(b)) suggests that both V_{A_8} (a deep donor) and Ga_{A_8} – V_{Ga} (a deep acceptor) contribute to the TSC signal at a temperature around 188 K and that T_3 is composed of two traps, one an electron trap resulting from V_{A_8} and the other a hole trap resulting from Ga_{A_8} – V_{Ga} . Neither can the possibility that oxygen may be involved [27, 28] in T_3 instead of V_{A_8} be excluded.

3.4. The effect of the starting temperature

Our TSC measurements were limited to the temperature range from 90-250 K, with the upper temperature limited by the rapid increase in the dark current, which is dominated by the ionization of the main deep donor EL2. Thus traps deeper than T_1 were not fully observed. The starting temperature from which the sample is rapidly cooled down to the lowest temperature (about 90 K) after a previous TSC measurement run has a significant effect on the resultant TSC spectra. Typical results for positive and negative biasing conditions are shown in Figs. 5(a) and 5(b). When the starting temperature is increased from 247 to 373 K, the ratios of the peak heights, i.e. T_3/T_2 in the positive bias case and T_3/T_1 in the negative bias case, increase. The ratios change basically because the increase in the starting temperature results in an increase in T₃ and decreases in T_2 and T_1 . The peak heights of T_5 and T_6 do not change with the starting temperature.

The behavior of T_3 is not understood and a possible interpretation is hindered by the suspicion that it may be a composite of two defects with the ability to trap both electrons and holes. However, the effect of the increased starting tem-

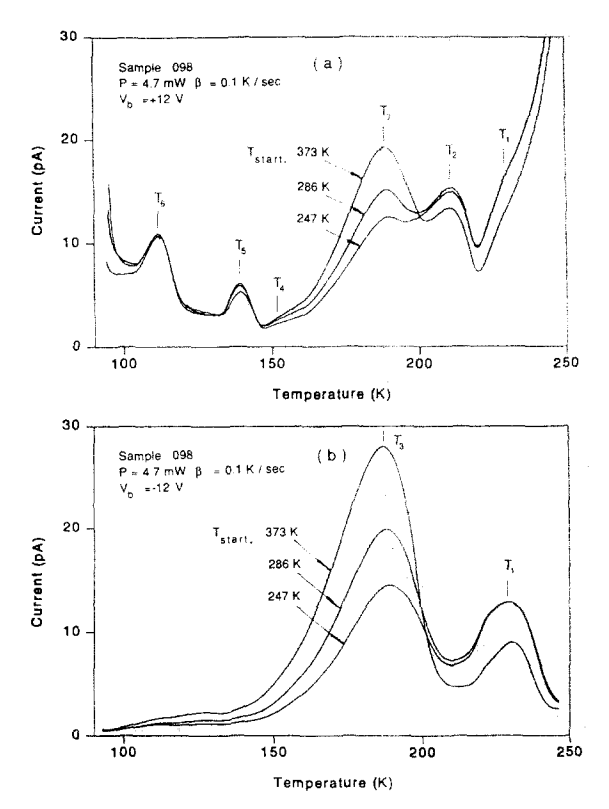


Fig. 5. The effect of holding the specimen at a high temperature (373 K) before rapid cooling to 90 K, and illumination, is to increase the height of the TSC peak for T_3 . The development of more arsenic vacancies might account for this effect, which is observed for both directions of voltage bias: (a) positive bias, (b) negative bias.

perature is to empty any traps that may be deeper than T_1 and to cause more and more ionization of EL2 ($T_{max} = 288 \text{ K}$) by transition from EL2⁰ to EL2⁺ and EL2⁺⁺. The effect of the starting temperature on the TSC spectra, *i.e.* on the T_3/T_2 and T_3/T_1 ratios, suggests that extra V_{As} can be created by the ionization of EL2, since T_3 is possibly related to V_{As} (from the discussion in the last section). Several antisite defect complex models such as $As_{Ga}V_{As}$ [29], $As_{Ga}V_{Ga}V_{As}$ [25], $As_{Ga}V_{As}V_{Ga}$ [30] and $As_{Ga}As_i$ [4] have been suggested for the atomic configuration of EL2 with As_{Ga} as the core.

The essence of the above suggestion is that the density of the trap T_3 is increased by the increased starting temperature. Alternatively, it may be that T_3 is of constant density and is merely more effectively filled by exposure to illumination at 90 K after sitting at starting temperatures in the range of 247-373 K. This, however, is hard to reconcile with the subsequent emission range 170-190 K in the TSC ramp.

Another speculation is that holding the specimen at 373 K allows the development of V_{As} by the creation of As_i , perhaps with condensation of As_i on dislocations, and the increased concentration of V_{As} -related defects then gives an increased T_3 signature. Whether an impurity such as oxygen contributes to this process is not known, although oxygen on the surface of GaAs is known to create free arsenic.

3.5. The effects of annealing

The TSC measurements were performed on three samples with different thermal histories. Sample 066 was taken from an as-grown SI-GaAs ingot grown from an arsenic-rich melt under high pressure. Sample 055, which was taken from the same ingot, was a siliconimplanted and activated sample but with the implanted layer removed by chemical etching. The implant conditions were Si²⁸, 150 keV and 3×10^{12} cm⁻², and the activation conditions were a capless anneal at 850 °C for 30 min in an arsenic overpressure ambient. Sample 066A, taken from the same wafer as sample 066, was subjected to annealing in a covered boat at 695 °C for 51 h under hydrogen flow in wafer proximity fashion, followed by fast cooling. The TSC spectral structures in Fig. 6 show that the anneal caused T_2 to increase with the ratio of T_3/T_2 decreasing and T_5 and T_6 to decrease. The effect of the long-term anneal may be explained in the following way. In as-grown SI-GaAs there exists a large concentration of V_{Ga} and V_{As} which behave as hole traps. As_{Ga}⁺⁺ and Ga_{As}V_{Ga} appear in the TSC spectrum at positive bias conditions as T_2 and T_3 . During long-term wafer anneal, several defect- or impurity-involved reactions, i.e. $V_{As} + Ga_{Ga} = Ga_{As} + V_{Ga}$, $V_{Ga} + As_i = As_{Ga}$, $V_{As} + As_i = As_{As}$ and $V_{Ga} + Cu_i = Cu_{Ga}$ can cause the annihilation of gallium and arsenic vacancies, since the existence of As, in as-grown SI-GaAs and the introduction of Cui during wafer annealing are easily understood. The fast cooling which follows the long annealing, tends to freeze the substituted atomic configurations formed during the annealing process. The net result is a decrease in the trap (T_3) which is $(Ga_{As}-V_{Ga})$ derived from V_{As} by a gallium hop, and an increase in the As_{Ga} related trap (T_2) . The decrease in T_5 and T_6 , which is accompanied by the decrease in T₃ and the increase in T_2 , further confirms that T_5 and T_6 are also vacancy related, as found in PITS studies [9]. In that work T_5 and T_6 are ascribed

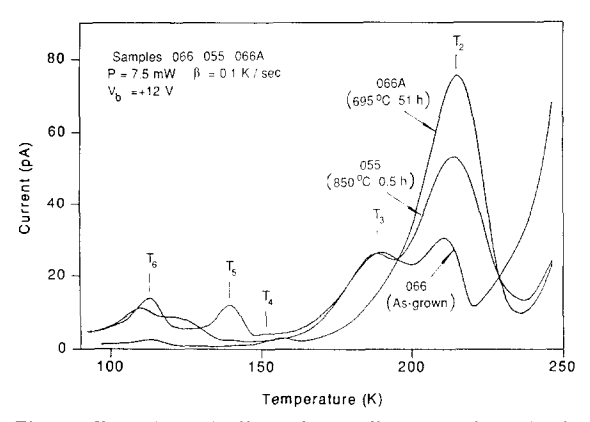


Fig. 6. The principal effect of annealing a specimen in the range $695\text{--}850\,^{\circ}\text{C}$ and susequent rapid cooling is the development of the hole trap peak T_2 at about $0.44\text{--}0.49\,^{\circ}\text{eV}$ above the valence band edge. This defect center may be As_{Ga} related.

to V_{Ga} and Ga_{As}^{--} respectively, since both of them can be created by the reaction $V_{As} + Ga_{Ga} = Ga_{As} + V_{Ga}$ through the nearest neighbor hopping of a gallium atom during the long-term illumination at 90 K. The photoluminescence spectra at 4.2 K for two proximityannealed SI-GaAs samples (066A and 098A) shown in Fig. 7 indicate some evidence of the occurrence of the GaAs and copper-related PL emissions. Before the 695 °C, 51 h anneal under hydrogen flow, the features that can be observed for both samples in the band edge region of the 4.2 K PL spectra, include the bound excitons at 1.512 and 1.514 eV, and the C_{As} features at 1.494eV (e- C_{As}) and 1.491 eV (D⁰- C_{As}) and the phonon replica at 1.457 eV (C_{As} + LO). However, after annealing, as can be seen from Fig. 7, new PL features appear with the bound exciton X_1 at 1.510 eV, the bound exciton X_2 at 1.508 eV, the Ga_{As}-related PL emission at 1.450 eV and the copper-related PL emissions at 1.345 and 1.360 eV. The appearance of the bound excitons (X_1) and X_2) and the Ga_{As} -related emissions is in agreement with the results reported by Yu et al. [31] in electrically reversible bulk GaAs annealed by 950 °C quenching or 950 °C slow cooling procedures. In contrast with their result two different copper-related emissions were observed with the 1.345 eV emission accompanied by a stronger 1.450 eV emission for sample (066A) grown by the HP-LEC technique and the 1.360 eV emission accompanied by a weaker 1.450 eV emission for sample (098A) grown by the LP-LEC technique. These observations are in agreement with our findings for annealed HB n-type GaAs [32]. The two copper-related emissions

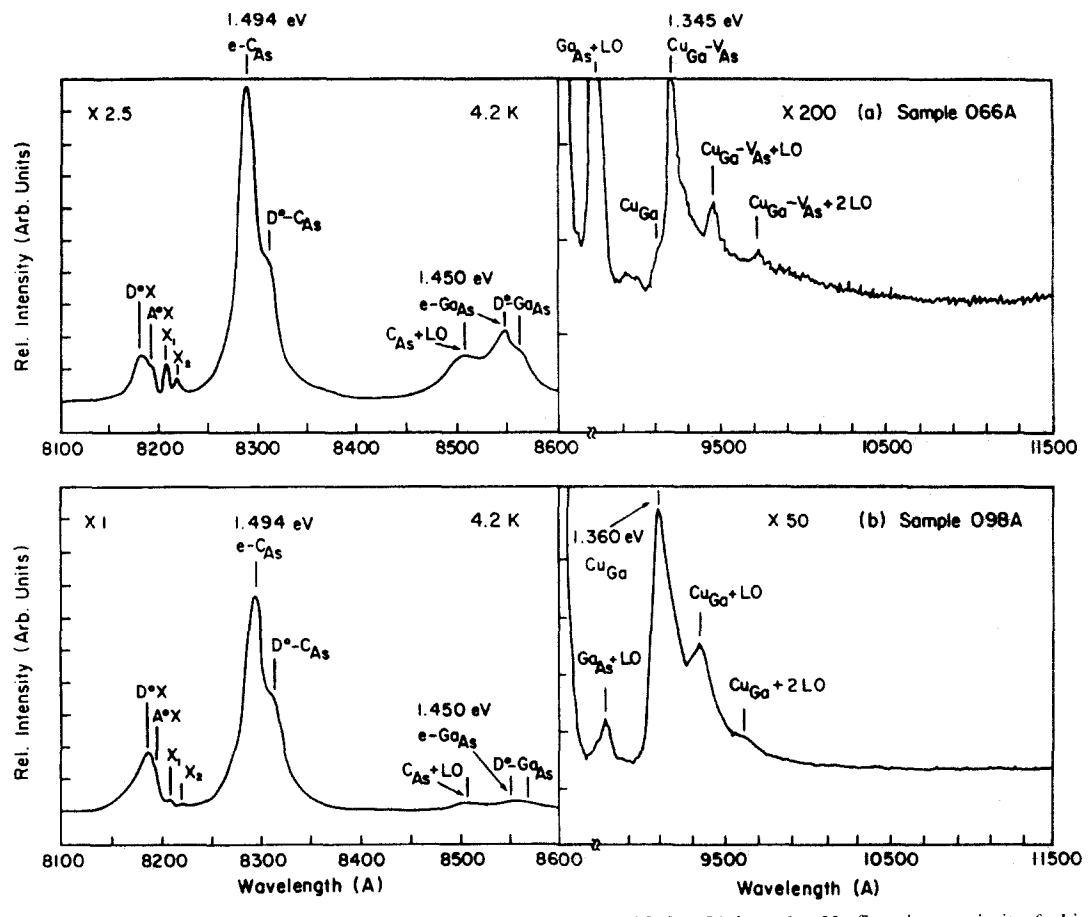


Fig. 7. Photoluminescence spectra of samples annealed at 695 °C for 51 h under H_2 flow in proximity fashion showing the occurrence of Ga_{A_1} and copper-related emissions and the difference in features of copper-related emissions for sample 066A (HP-LEC grown) and sample 098A (LP-LEC grown).

with different intensities of the accompanying 1.450 eV emission imply a different defect structure in as-grown SI-GaAs produced by HP- and LP-LEC techniques.

3.6. Further comparison of as-grown and annealed SI-GaAs

To further our understanding of the possible nature of the main traps $(T_2, T_3, T_5 \text{ and } T_6)$ observed in TSC spectra and to help elucidate the photocurrent enhancement photo-induced **PITS** studies [9],the observed in measurements were performed with changes of the light intensities and the illumination times on two different samples—one an as-grown SI-GaAs (066) specimen and the other an annealed (695 °C, 51 h) SI-GaAs (066A) specimen (both of them taken from same wafer). During the illumination at 90 K, the photocurrent responses were also measured for the two samples.

3.6.1. The effect of light intensity

Figures 8(a) and 8(b) present the photocurrent responses at different light intensities for the asgrown sample (066) and the annealed sample (066A) respectively. As can be seen from Fig. 8(a) a "two-plateau" structure with the time duration of the first plateau inversely proportional to the light intensity can be observed. However, no such "two-plateau" structure can be observed on the annealed SI-GaAs (Fig. 8(b)). The difference in the behavior of the photocurrent response reflects the difference in defect constitution. Figures 9(a) and 9(b) show the TSC spectra with long-term illumination at 90 K (greater than 10 min) at different light intensities for the two samples. As can be seen from Fig. 9(a), the peak height of T₅ is gradually increased by increasing the light intensity, as compared with the other traps $(T_2, T_3 \text{ and } T_6)$. However, from Fig. 9(b) no such development can be observed for any traps,

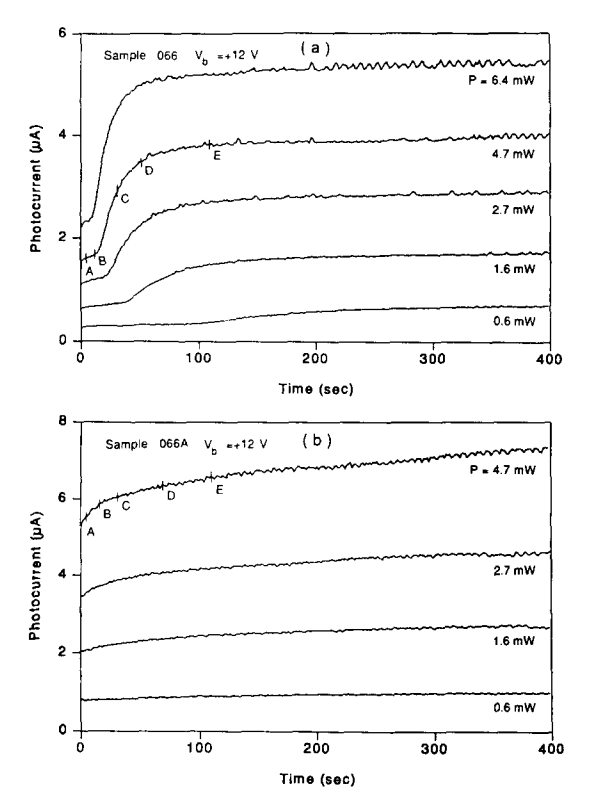


Fig. 8. Photocurrent responses with time for various light intensities (1.96 eV, 0.6-6.4 mW). In (a) for the as-grown sample (066) a two-plateau structure is observed. In (b) for the wafer annealed sample (066A) the initial plateau is absent.

except for some feature changes around 90 K. This result indicates that the photocurrent enhancement behavior (*i.e.* two-plateau structure in photocurrent response) might be related to the development of some traps, including T_5 , as suggested in previous PITS studies [9].

3.6.2. The effect of the illumination time

TSC measurements were performed with different illumination times ranging from 5 s to about 110 s which correspond to transition times from the first plateau to the second plateau in the photocurrent response, labeled A, B, C, D and E in Figs. 8(a) and 8(b) (although without a "two-plateau" structure in Fig. 8(b)). These TSC results are shown in Fig. 10(a) and 10(b). For the asgrown SI-GaAs sample, Fig. 10(a), the increasing illumination time results in (1) the development of the peak heights of T₂, T₄, T₅ and T₆, (2) almost no change in peak height for T₃, but a peak shift to higher temperature, and (3) a decrease in the peak height of T₇ and T₅*. However,

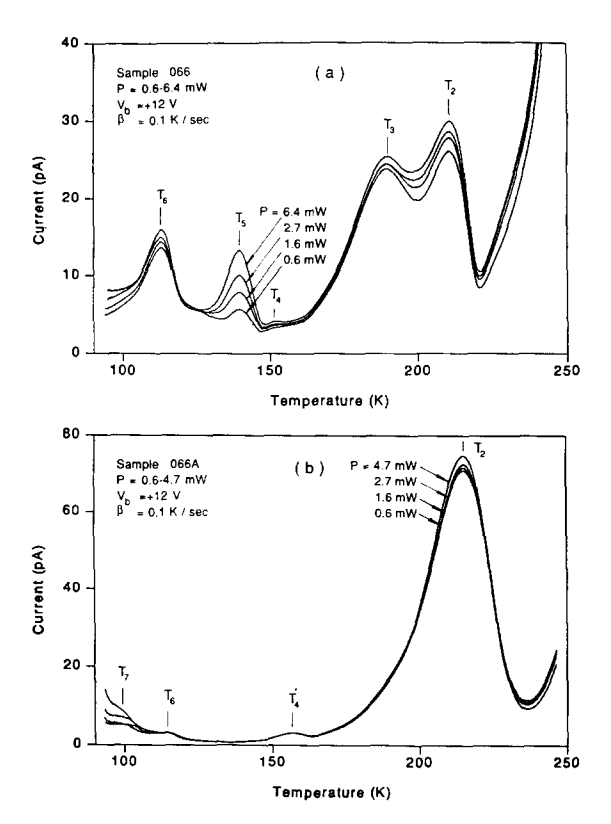
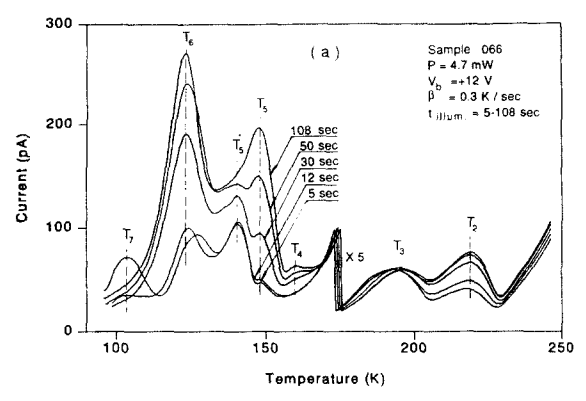


Fig. 9. Effects of varying light intensity on the TSC spectra. In (a) for the as-grown specimen, 066, the peak T_5 is seen to increase with increase in light intensity and there is also a change in T_2 . However, after annealing (b) (specimen 066A) the peaks T_6 and T_5 have been suppressed and T_3 is lost in the shoulder of T_2 , which has almost doubled in concentration. It is possible that T_3 has been formed by arsenic interstitials entering vacant gallium sites.

for the annealed SI-GaAs sample, Fig. 10(b), increasing illumination time results in only the same increase in peak height for all traps with no suppression. The relative increases in peak heights for T_2 , T_5 and T_6 in the as-grown SI-GaAs sample are much larger than those in the annealed SI-GaAs sample. To explain the difference in the photocurrent response at 90 K and in the TSC spectra with increasing illumination time for the two samples with different thermal history, we suggest a mechanism of reversible photoinduced defect reactions, as responsible for the change in the trap and the recombination center by illumination at low temperature, rather than offering a mechanism which is associated only with increased carrier trapping [33, 34]. An increased carrier trapping mechanism cannot readily explain the suppression of some traps (T₇ and T₅*) and the absence of any change in trap T₃. Differences in hole capture cross-section



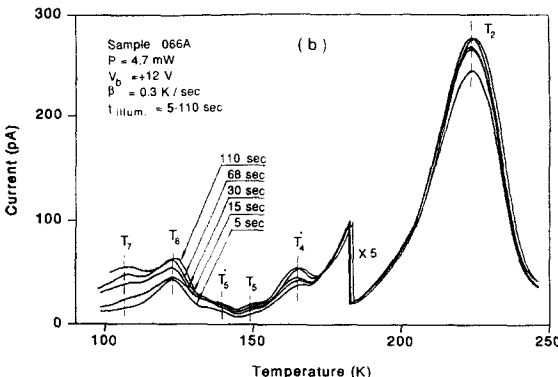


Fig. 10. The TSC spectra show the effects of varying illumination time at 90 K from 5 to 110 s: (a) as-grown specimen 066, (b) similar material (066A) after a 695 °C anneal in $\rm H_2$. Traps $\rm T_5$ and $\rm T_6$ are seen to be reduced by the anneal and $\rm T_2$ greatly increased. Increased illumination may be doing something more to the concentrations of traps $\rm T_5$ and $\rm T_6$ than merely increasing their filling ratio.

might be involved, but they are expected to be of nearly the same order $(10^{-15}\text{-}10^{-14}~\text{cm}^2)$, from cross-section measurements for HM1 (As_{Ga}⁺⁺), HL5 (Level A in LPE-GaAs) and HL12, HB6 or H1 (V_{Ga}-related) and the probability that T_2 , T_3 and T_5 are related to these traps studied earlier in doped GaAs.

Although the detailed processes and equilibria of the photo-induced defect reactions are unknown at present, it seems that the related defects include the main intrinsic point defects: V_{As} , V_{Ga} , Ga_{As} , As_{Ga} and As_i and the complexes associated with them. The following reactions could be involved

$$[V_{As} - V_{Ga}] = V_{As}(T_3) + V_{Ga}(T_5)$$
(6)

$$V_{As} + Ga_{Ga} = Ga_{As}(T_6) + V_{Ga}(T_5)$$
 (7)

$$V_{As} + Ga_{Ga} = [Ga_{As} - V_{Ga}](T_3)$$
 (8)

$$V_{Ga} + As_i = As_{Ga}(T_2) \tag{9}$$

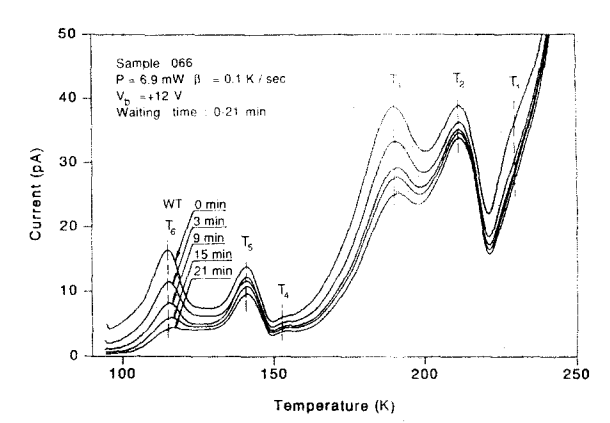


Fig. 11. These spectra show the effect of waiting time (0-21 min) on specimen 066 between turn-off of illumination at 90 K and the start of the TSC temperature ramp. From the variation of the peak height of T_6 it is possible to estimate a capture cross-section of 5×10^{-17} cm² for the process $Ga_{As}^- + e_{VB} \longrightarrow Ga_{As}^{2-} + p$.

Before illumination, some intrinsic point defects complex with each other, for example to create $[V_{As}-V_{Ga}]$, which could play a role in recombination action, but after long-term illumination the center may be separated into individual point defects, causing photocurrent enhancement at 90 K and the development of related traps $(T_2, T_5 \text{ and } T_6)$.

However, for the SI-GaAs which experienced a long-term anneal, the vacancy-related point defects, such as V_{As} or V_{As} – V_{Ga} , are already annihilated by the mobile species (As_i and/or Cu_i). Therefore no photoinduced defect reactions would be expected and the carrier trapping mechanism might dominate the illumination process. From this point of view, the long-term annealed SI-GaAs material is more stable than the as-grown SI-GaAs material.

3.7. The effect of the waiting time

In TSC spectroscopy not all of the carriers captured by a trap will be released unless the temperature is raised past the peak temperature, corresponding to the maximum trap emission current. The thermal cleaning technique used in TSC measurements is based on this principle. As can be seen in Fig. 11, the waiting time at 90 K, *i.e.* the time between interrupting the illumination and starting the thermal scan, affects the peak height of T₃ and T₆. The T₆ peak we believe is related to the emission of holes to the valence band by the reaction

$$Ga_{As}^{-} + e_{VB} \longrightarrow Ga_{As}^{--} + p \tag{10}$$

This process is at its peak at a temperature of

about 113–115 K and corresponds to a trap activation energy of $E_v + 0.21$ eV (obtained either from an Arrhenius plot or from the initial rise technique) [35]. However, this emission is taking place at a slow rate during the waiting time at 90 K and

$$I_{\rm TSC} = \frac{\mathrm{d}p}{\mathrm{d}t} = e_{\rm p}(90 \text{ K}) N(t)_{\rm Ga_{Ac}}$$
 (11)

where $e_p(90 \text{ K})$ is the emission rate at 90 K and $N(t)_{\text{Ga}_{As}}$ is the concentration of the trap Ga_{As} at time t. The emission coefficient we assume to be given by

$$e_{\rm p} = \sigma_{\rm p} v_{\rm th} N_{\rm v} \exp(-0.21/kT) \tag{12}$$

where $\sigma_{\rm p}$ is the capture cross-section (at T), $v_{\rm th}$ is the thermal velocity at T, and $N_{\rm v}$ is the effective density of states of the valence band. The holes (density) emitted in time Δt are equal to $-\Delta N_{\rm Ga_{\rm Av}}$ from eqn. (10). Hence

$$\frac{1}{N(t)} dN(t) = -e_{\rm p} dt \tag{13}$$

and so

$$N(t) = N(t = 0)(1 - \exp(-e_{p}t))$$
 (14)

When the charge emitted for peak T_6 is plotted as a function of time the slope obtained is 9×10^{-4} s⁻¹ corresponding to a characteristic time at 90 K of 1100 s. This time constant is even more readily obtained by plotting the height of the T_6 peak vs. waiting time t_w . Equation (12) then yields 5×10^{-17} cm² for $\sigma_p(90 \text{ K})$. This is a plausible value for a process involving the capture of a second electron. An independent determination, for comparison, has not been found in the literature

It may be noted that for the first-electron capture process

$$Ga_{As}^{0} + e_{VB} \longrightarrow Ga_{As}^{-} + p \tag{15}$$

a study [36] has shown σ_{∞} to be 7.1×10^{-15} cm⁻³

$$\sigma_{\rm p} = 7.1 \times 10^{-15} \exp(-0.050/kT)$$
 (16)

hence $\sigma_{\rm p}(90~{\rm K})$ for ${\rm Ga_{As}}^{0/-}$ is inferred to be $1.1\times 10^{-17}~{\rm cm^2}$, which is not too dissimilar from our value for second-electron capture.

Peak T₃ has been studied by a similar technique after cleaning traps discharging at lower temperatures and then maintaining the tempera-

ture at 160 K before starting the TSC scan. The slope of the rising edge of current [35] then gave an energy level of 0.42 eV, which matched the 0.44 eV that was obtained with an Arrhenius plot and is close to the 0.39 eV given in Table 2 obtained from eqn. (5). By variation of the waiting time at 160 K, in the range 1–35 min, the capture cross-section of T_3 at 160 K was estimated to be 3×10^{-16} cm² assuming T_3 is an electron trap (or 5 times smaller if T_3 is a hole trap).

4. Conclusions

TSC spectroscopy has been used to characterize the traps in SI-GaAs. At least six traps can be observed in the temperature range from 90 to 240 K using basic measurement conditions, i.e. excitation light of 1.96 eV, a sufficiently long illumination time (greater than 10 min) and an average heating rate of 0.1 K s⁻¹. By changing the bias polarity, T_1 is assigned to an electron trap, T_2 , T_4 , T_5 and T_6 are assigned to hole traps and T_3 might be related to both hole and electron trapping action. The energy levels for T_2 , T_3 , T_5 , T_6 are 0.49 eV, 0.44 eV, 0.26 eV and 0.21 eV respectively, determined by Arrhenius plots of nT_m^2/β vs. $1/T_{\rm m}$. These values are close to the energy levels calculated using the approximate equation $E_i = kT_m n T_m^4/\beta$. The densities of the main traps $(T_2, T_3, T_5 \text{ and } T_6)$ are in the range of mid-10¹⁵ to 10^{17} cm⁻³, which are not easily accounted for by residual metal impurities, such as copper, iron, manganese etc. Through comparison of the TSC spectra for samples with different stoichiometry and different thermal history, T_2 , T_3 , T_5 and T_6 are tentatively identified as $As_{Ga}^{\ +\ +}$, $Ga_{As}V_{Ga}$ (or V_{As}), V_{Ga} and Ga_{As}^{--} respectively. By further studying the effect of the light intensity and the illumination time on the TSC spectra obtained from an as-grown and an annealed SI-GaAs sample a mechanism of photo-induced defect reaction is suggested to interpret the two-plateau structure in the photocurrent response at 90 K. The defect reactions during illumination might be associated with the vacancy-related defects, such as $V_{As}-V_{Ga}$ and V_{As} , and the hopping mechanism of nearest neighbor Ga and As, atoms.

Acknowledgments

This work was supported in part by the Solar Energy Research Institute under contract number XB-6-06005-3 and by the Army Research Office

under contract number DAAL 03-86-1K-0066. We thank David Wong for his skilful computer assistance and also P. J. Pearah for valuable discussions.

References

- E. R. Weber and M. Kaminska. In G. Grossmann and L. Ledebo (eds.), *Proc. 5th Conf. on Semi-insulating III-V Materials*, *Malmo*, *1988*, Adam Hilger, Bristol, 1988, p. 111
- 2 A. T. Hunter. In E. R. Weber (ed.), Defect Recognition and Image Processing in III-V Compounds II, Elsevier, 1987, p. 137.
- 3 S. Miyazawa, Defects in semiconductors I. In H. J. vonBardeleben (ed.), *Materials Science Forum*, Vol. 10–12, pt. 1, TransTech, Aedermansdorff, 1986, p. 1.
- 4 J. C. Bourgoin and H. J. vonBardeleben, J. Appl. Phys., 64 (R65) (1988).
- 5 D. C. Look. In G. Grossmann and L. Ledebo (eds.), Proc. 5th Conf. on Semi-insulating III-V Materials, Malmo, 1988, Adam Hilger, Bristol, 1988, p. 1.
- 6 J. Blanc, R. H. Bube and L. R. Weisberg, J. Phys. Chem. Solids, 25 (1964) 225.
- 7 W. Kuszko, P. J. Walczak, P. Trautman, M. Kaminska and J. M. Baranowski, Defects in semiconductors I. In H. J. vonBardeleben (ed.), *Materials Science Forum*, Vol. 10–12, pt. 1, TransTech, Aedermansdorff, 1986, p. 317.
- M. Tomozane, Y. Nannichi, H. Kamada and K. Ando, *Jpn. J. Appl. Phys.*, 26 (L1076) (1987).
- 9 Z.-Q. Fang, L. Shan, T. E. Schlesinger and A. G. Milnes, *Solid State Electron*, 32 (1989) 405.
- 10 P. J. Pearah, R. Tobin, J. P. Tower and R. M. Ware. In G. Grossmann and L. Ledebo (eds.), Proc. 5th Conf. on Semi-insulating III-V Materials, Malmo, 1988, Adam Hilger, Bristol, 1988, p. 195.
- 11 G. M. Martin and D. Bois, *Electrochem. Soc. Ext. Abstr.*, 78–3 (1978) 32.
- 12 M. Tomozane and Y. Nannichi, Jpn. J. Appl. Phys., 25 (L273)(1986).
- 13 R. H. Bube, *Photoconductivity of Solids*, Wiley, New York, 1960.
- 14 D. C. Look, Semicond. Semimetals, 19 (1983) 75.
- 15 A. L. Lin, E. Omelianovski and R. H. Bube, *J. Appl. Phys.*, 47 (1976) 1852.
- 16 A. L. Lin and R. Bube, J. Appl. Phys., 47 (1976) 1859.

- 17 G. M. Martin, A. Mitonneau and A. Mircea, *Electron. Lett.*, *13* (1977) 191.
- 18 A. Mitonneau, G. M. Martin and A. Mircea, *Electron. Lett.*, *13* (1977) 666.
- 19 J. Krauskopf, J. D. Meyer, B. Wiedemann, M. Waldschmidt, K. Bethge, G. Wolf and W. Schutze. In G. Grossmann and L. Ledebo (eds.), Proc. 5th Conf. on Semi-insulating III-V Materials, Malmo, 1988, Adam Hilger, Bristol, 1988, p. 165.
- 20 R. A. Morrow, J. Mater. Res., 2 (1987) 681.
- 21 S. Reichlmaier, K. Lohnert and M. Baumgartner, *Jpn. J. Appl. Phys.*, 27 (1988) 2329.
- 22 D. Pons and J. C. Bourgoin, J. Phys. C, 18 (1985) 3839.
- 23 J. Lagowski, D. G. Lin, T. P. Cheng, M. Skowronski and H. C. Gatos, *Appl. Phys. Lett.*, 97 (1985) 929.
- 24 R. N. Thomas, H. M. Hobgood, G. W. Eldridge, D. L. Baratt, T. T. Braggins, L. B. Ta, and S. K. Wang. In R. K. Willardson and A. C. Beer (eds.), *Semicond. Semimetals*, Vol. 20, Academic, Orlando, FL, 1984, p. 1.
- 25 J. F. Wagner and J. A. Van Vechten, *Phys. Rev.*, *B35* (1987) 2330.
- 26 G. A. Baraff and M. Schluter, *Phys. Rev.*, *B33* (1986) 7346.
- 27 H. Ch. Alt, Appl. Phys. Lett., 54 (15) (1989) 1445.
- 28 J. Schneider, B. f. Dischler, H. Seelewind, P. M. Mooney, J. Lagowski, M. Matsui, D. R. Beard and R. C. Newman, Appl. Phys. Lett., 54 (15) (1989) 1442.
- 29 J. Lagowski, M. Kaminska, J. M. Parsey, H. C. Gatos and W. Walukiewicz. In *Proc. Inst. Phys. Conf. on GaAs and Related Compounds*, 1982, Ser. No. 65, p. 41.
- 30 G. Wang, Y. Zou, A. Goltzene, B. Meyer and C. Schwab. In G. Grossmann and L. Ledebo (eds.), *Proc. 5th Conf. on Semi-insulating III-V Materials*, *Malmo*, *1988*, Adam Hilger, Bristol, 1988, p. 387.
- 31 P. W. Yu, D. C. Look and W. Ford, *J. Appl. Phys.*, 62 (7) (1987) 2960.
- 32 Z. Q. Fang, L. Shan, J. H. Zhao, X. J. Bao, T. E. Schlesinger and A. G. Milnes, *J. Electron. Mater.*, 18 (2) (1989) 123.
- 33 M. Tomozane, Y. Nannichi, I. Onodera, T. Fukase and F. Hasegawa, Jpn. J. Appl. Phys., 27 (1988) 260.
- 34 U. V. Desnica and B. Santic, Appl. Phys. Lett., 54 (1989) 810
- 35 A. G. Milnes, *Deep Impurities in Semiconductors*, Wiley, New York, 1973, Chapter 9, p. 236.
- 36 P. W. Yu, W. C. Mitchel, M. G. Mier, S. S. Li and W. L. Wang, Appl. Phys. Lett., 41 (6) (1982) 532.